PHYSICAL REVIEW D **80,** 033002 (2009)

Probing nonunitary mixing and *CP* violation at a neutrino factory

Stefan Antusch,* Mattias Blennow,† and Enrique Fernandez-Martinez‡
Max-Planck-Institut für Physik (Werner-Heisenberg-Institut), Föhringer Ring 6, 80805 München, Germany

Jacobo López-Pavón§
Instituto de Física Teórica UAM/CSIC, Universidad Autónoma de Madrid, 28049 Cantoblanco, Madrid, Spain
(Received 21 April 2009; published 11 August 2009)

A low-energy nonunitary leptonic mixing matrix is a generic feature of many extensions of the standard model. In such a case, the task of future precision neutrino oscillation experiments is more ambitious than measuring the three mixing angles and the leptonic (Dirac) *CP* phase, i.e., the accessible parameters of a unitary leptonic mixing matrix. A nonunitary mixing matrix has 13 parameters that affect neutrino oscillations, out of which four are *CP* violating. In the scheme of minimal unitarity violation we analyze the potential of a neutrino factory for determining or constraining the parameters of the nonunitary leptonic mixing matrix, thereby testing the origin of *CP* violation in the lepton sector.

DOI: 10.1103/PhysRevD.80.033002 PACS numbers: 14.60.Pq, 14.60.St

I. INTRODUCTION

There are several indications from particle physics, as well as from cosmology, for the existence of physics beyond the standard model (SM). For example, the gauge hierarchy problem suggests that new physics exists at energies close to the electroweak scale in order to stabilize it against large quantum corrections. In cosmology, the evidence for dark matter in the Universe requires the extension of the SM particle content. Last, but not least, the discovery that neutrinos are massive provides the first clear particle physics evidence that the SM has to be extended.

In general, extensions of the SM will also affect the physics relevant at neutrino oscillation experiments. New physics effects on neutrino oscillations are particularly relevant for the next generation of precision neutrino oscillation facilities such as neutrino factories [1,2], which aim at measuring the unknown leptonic mixing angle θ_{13}, the neutrino mass hierarchy [i.e., $\mathrm{sgn}(\Delta m^2_{31})$], as well as the Dirac phase δ, which can induce *CP* violation in neutrino oscillations. In most phenomenological studies regarding the sensitivities of future neutrino oscillation facilities, the leptonic mixing matrix is assumed to be unitary.

In contrast to this common practice, it is well known that one generic feature of new physics in the lepton sector is the nonunitarity of the low-energy leptonic mixing matrix. This nonunitarity appears whenever additional heavy particles mix with the light neutrinos or their charged lepton partners [3–28]. After integrating the heavy states out of the theory, the 3×3 submatrix of the light neutrinos remains as an effective mixing matrix. This low-energy leptonic mixing matrix is, in general, not unitary.

While there are many models of physics beyond the SM which induce nonunitarity, an extension of the SM featuring a nonunitary leptonic mixing can be described in a minimal way through an effective theory, the so-called *Minimal Unitarity Violation (MUV)* scheme [19]. It contains the relevant low-energy information for neutrino oscillation experiments and is minimal in the sense that only three light neutrinos are considered and that new physics is introduced in the neutrino sector only. It provides an effective description of all models where additional heavy singlets mix with three light neutrinos.[1]

In MUV, the charged- and neutral-current interactions of the neutrinos (i.e., their couplings to the W and Z bosons) are modified. The nonunitary leptonic mixing matrix N, which appears in the charged-current interaction, contains the only additional degrees of freedom, since the neutral-current interaction of the neutrinos is proportional to $N^\dagger N$ while the neutral-current interaction of the charged leptons is unchanged. Thus, instead of the three mixing angles and three *CP* phases of a unitary leptonic mixing matrix (with only one affecting neutrino oscillations), the nonunitary mixing matrix N contains 15 parameters, out of which six are *CP*-violating phases (including two Majorana phases, which do not affect neutrino oscillations).

In this study, we investigate the potential of a neutrino factory for determining or constraining the parameters of the nonunitary leptonic mixing matrix, thereby testing the origin of *CP* violation in the lepton sector.

*antusch@mppmu.mpg.de
†blennow@mppmu.mpg.de
‡enfmarti@mppmu.mpg.de
§jacobo.lopez@uam.es

[1]Other possibilities to introduce nonunitary leptonic mixing are, e.g., via an additional vectorlike lepton generation or via fermionic $SU(2)_L$ triplets, which are beyond MUV. Nonunitarity in these schemes turns out to be significantly more constrained by nonoscillation experiments than in MUV (see, e.g., Ref. [20]).

II. GENERAL INTRODUCTION TO UNITARITY VIOLATION

As motivated in the introduction, nonunitarity of the leptonic mixing matrix is a generic manifestation of new physics in the lepton sector. The MUV scheme provides an effective field theory extension of the SM and is minimal in the sense that only three light neutrinos are considered and that new physics is only introduced in the neutrino sector. Notice that this assumption is conservative, since new physics affecting other sectors, such as that of the charged leptons, will lead to stronger signals than the ones discussed here. The MUV scheme thus describes the relevant effects on neutrino oscillations in the various types of models where the SM is extended by heavy singlet fermions (where "heavy" refers to large masses compared to the energies of the neutrino oscillation experiments) which mix with the light neutrinos.

In the MUV scheme, the Lagrangian density of the SM is extended by two effective operators, one of mass dimension five and one of mass dimension six. The dimension five operator is the ubiquitous lepton number violating Weinberg operator $\delta\mathcal{L}^{d=5} = \frac{1}{2} c_{\alpha\beta}^{d=5} (\bar{L}^c{}_\alpha \tilde{\phi}^*)(\tilde{\phi}^\dagger L_\beta) +$ H.c., the lowest dimensional effective operator for generating neutrino masses using the field content of the SM. The coefficient matrix $c_{\alpha\beta}^{d=5}$ is of $\mathcal{O}(1/M)$ and related to the low-energy neutrino mass matrix by $m_\nu = v_{\mathrm{EW}}^2 c^{d=5}$, where v_{EW} is the vacuum expectation value of the SM Higgs field ϕ, which breaks the electroweak symmetry, and $\tilde{\phi} = i\tau_2 \phi^*$. The SM neutrinos are contained in the lepton doublets L_α, with $\alpha = e, \mu, \tau$ running over the three families.

The effective dimension six operator $c_{\alpha\beta}^{d=6} (\bar{L}_\alpha \tilde{\phi}) i\not{\partial} (\tilde{\phi}^\dagger L_\beta)$ conserves lepton number[2] and, after electroweak symmetry breaking, contributes to the kinetic terms of the neutrinos. After their canonical normalization, they generate a nonunitary leptonic mixing matrix N, as well as nonuniversal couplings of the neutrinos to the Z boson proportional to $N^\dagger N$. The modified part of the Lagrangian density in MUV is given by

$$\begin{aligned}\mathcal{L}^{\mathrm{eff}} = & \frac{1}{2}(\bar{\nu}_i i\not{\partial}\nu_i - \bar{\nu^c}_i m_i \nu_i + \mathrm{H.c.}) \\ & - \frac{g}{2\sqrt{2}}(W_\mu^- \bar{l}_\alpha \gamma_\mu (1-\gamma_5) N_{\alpha i} \nu_i + \mathrm{H.c.}) \\ & - \frac{g}{2\cos\theta_W}(Z_\mu \bar{\nu}_i \gamma^\mu (1-\gamma_5)(N^\dagger N)_{ij} \nu_j + \mathrm{H.c.}).\end{aligned} \tag{1}$$

We note that the MUV scheme is also minimal in the sense that all new physics effects depend on the nonunitary leptonic mixing matrix N. Regarding neutrino oscillation experiments, the nonunitarity of N affects the processes at the source and the detector as well as neutrino propagation in matter.

To parametrize N, we use the fact that a general matrix can be written as the product of a Hermitian matrix times a unitary matrix. Decomposing the Hermitian matrix as $\mathbb{1} + \varepsilon$ (with $\varepsilon = \varepsilon^\dagger$) and denoting the unitary matrix by U, we can write [21]

$$N = (\mathbb{1} + \varepsilon) U. \tag{2}$$

For the complex off-diagonal elements of the matrix ε, we use the notation $\varepsilon_{\alpha\beta} = |\varepsilon_{\alpha\beta}| e^{i\phi_{\alpha\beta}}$. Notice that, due to the Hermiticity of ε, $|\varepsilon_{\alpha\beta}| = |\varepsilon_{\beta\alpha}|$, and $\phi_{\alpha\beta} = -\phi_{\beta\alpha}$. The diagonal elements are real and no further parametrization is required. Constraints on the $\varepsilon_{\alpha\beta}$ can also be derived from the experimental data on electroweak decays [11,12]. The present 90% CL bounds are $|\varepsilon_{\mu e}| < 3.5 \cdot 10^{-5}$, $|\varepsilon_{\tau e}| < 8.0 \cdot 10^{-3}$, $|\varepsilon_{\tau\mu}| < 5.1 \cdot 10^{-3}$ [19], and $|\varepsilon_{ee}| < 2.0 \cdot 10^{-3}$, $|\varepsilon_{\mu\mu}| < 8.0 \cdot 10^{-4}$, $|\varepsilon_{\tau\tau}| < 2.7 \cdot 10^{-3}$ [25]. In our analysis, we will consider unitarity violation consistent with the present bounds. Analytic expressions for the neutrino oscillation probabilities in terms of U and ε can be found in Appendix A.

Finally, we would like to comment on other possible parametrization of a nonunitary leptonic mixing matrix. In Refs. [15,22,23,27], a different parametrization is advocated, in which the deviations from unitarity of the mixing matrix involving the three light neutrinos is related to the mixing between these light neutrinos and the heavy singlets in seesaw type theories. The mixing matrix in a seesaw scenario is the unitary matrix that diagonalizes the extended neutrino mass matrix:

$$U_{6\times 6}^T \begin{pmatrix} 0 & m_D \\ m_D^T & M_N \end{pmatrix} U_{6\times 6} = \begin{pmatrix} m & 0 \\ 0 & M \end{pmatrix}, \tag{3}$$

where m_D and M_N are the neutrino's Dirac and Majorana mass matrices, respectively. In the case of only one neutrino family, the unitary matrix is just a rotation of angle $\theta \simeq m_D/M$. The extension to three or more families is straightforward, performing the diagonalization in two steps: first a block-diagonalization and then two unitary rotations to diagonalize the mass matrices of the light and heavy neutrinos, i.e.,

$$U_{6\times 6} = \begin{pmatrix} A & B \\ C & D \end{pmatrix} \begin{pmatrix} U & 0 \\ 0 & V \end{pmatrix}, \tag{4}$$

where U and V are unitary matrices. Without loss of generality, we can choose a basis for the heavy singlets such that $V = I$. Analogously to the one family example, when performing the block-diagonalization, the mixing between the light and heavy neutrinos is suppressed so that

$$B \simeq \Theta = m_D M_N^{-1}. \tag{5}$$

This suppression is exploited in Refs. [23,27], where the

[2]We note that since the dimension six operator conserves lepton number, it is not necessarily suppressed by the smallness of the neutrino masses.

block diagonalizing matrix is written as the product of the 9 possible rotations mixing the light and heavy states and then expanded up to second order in the small mixing angles. This results in

$$A = 1 - \begin{pmatrix} \frac{1}{2}(s_{14}^2 + s_{15}^2 + s_{16}^2) & 0 & 0 \\ \hat{s}_{14}\hat{s}_{24}^* + \hat{s}_{15}\hat{s}_{25}^* + \hat{s}_{16}\hat{s}_{26}^* & \frac{1}{2}(s_{24}^2 + s_{25}^2 + s_{26}^2) & 0 \\ \hat{s}_{14}\hat{s}_{34}^* + \hat{s}_{15}\hat{s}_{35}^* + \hat{s}_{16}\hat{s}_{36}^* & \hat{s}_{24}\hat{s}_{34}^* + \hat{s}_{25}\hat{s}_{35}^* + \hat{s}_{26}\hat{s}_{36}^* & \frac{1}{2}(s_{34}^2 + s_{35}^2 + s_{36}^2) \end{pmatrix} + \mathcal{O}(\theta_{ij}^4),$$
$$B = \begin{pmatrix} \hat{s}_{14}^* & \hat{s}_{15}^* & \hat{s}_{16}^* \\ \hat{s}_{24}^* & \hat{s}_{25}^* & \hat{s}_{26}^* \\ \hat{s}_{34}^* & \hat{s}_{35}^* & \hat{s}_{36}^* \end{pmatrix} + \mathcal{O}(\theta_{ij}^3), \tag{6}$$

where $\hat{s}_{ij} = s_{ij}\exp(i\delta_{ij})$ and $s_{ij} = \sin(\theta_{ij})$. Notice that the mixing matrix of the three light neutrinos is given by $N = AU$. Thus, the deviation from unitarity, encoded in A, is directly related to the mixing B between the heavy and light neutrinos. We argue that this is also the case with the Hermitian unitarity deviation adopted in Eq. (2). Indeed, we can exploit the suppression of Eq. (5) to write the unitary block-diagonalization as the exponential expansion of an anti-Hermitian matrix:

$$\begin{pmatrix} A & B \\ C & D \end{pmatrix} = \exp\begin{pmatrix} 0 & \Theta \\ -\Theta^\dagger & 0 \end{pmatrix} = \begin{pmatrix} 1 - \frac{1}{2}\Theta\Theta^\dagger & \Theta \\ -\Theta^\dagger & 1 - \frac{1}{2}\Theta^\dagger\Theta \end{pmatrix} + \mathcal{O}(\Theta^3). \tag{7}$$

Thus, the Hermitian deviation from unitarity defined in Eq. (2) is just $\varepsilon = -\Theta\Theta^\dagger/2$ and its relation to the mixing between light and heavy neutrinos in a seesaw scenario is straightforward.[3] Furthermore, notice that the deviation from unitary mixing parametrized as in Eq. (6) can only be applied to the specific case of the mixing between three light and three heavy neutrinos while the product of an Hermitian and a unitary matrix is a completely general matrix and thus suitable to take into account more general scenarios. In addition, the unitarity deviation ε is given by the coefficient of the $d = 6$ operator ($\varepsilon = -c^{d=6}/2$) that modifies the neutrino kinetic terms, introduced in the MUV scheme and obtained in the effective theory of the seesaw mechanism after integrating out the heavy singlets (see, e.g., Ref. [29]).

III. NUMERICAL SIMULATION AND RESULTS

We will now discuss the sensitivity of future neutrino oscillation experiments to the different parameters of the MUV scheme. In particular, we study the ''standard'' neutrino factory setup proposed in the international design study (IDS) [30,31], which consists of ν_e and ν_μ beams from 5×10^{20} muon decays per year per baseline. We consider a setting where the experiment is assumed to run for five years in each polarity. The parent muons are assumed to have an energy of 25 GeV. The beams are detected at two far sites, the first located at 4000 km with a 50 kton magnetized iron neutrino detector (MIND) [32] and a 10 kton emulsion cloud chamber (ECC) for τ detection [33,34], and the second located close to the magic baseline [35,36] at 7500 km with an iron detector identical to the one at 4000 km.

Since our main interest is the sensitivity of the standard setup to nonunitarity, the only deviation from this standard setup that we will consider is the addition of a near detector at 1 km capable of ν_τ detection. In this sense, even if the experimental setup of the IDS neutrino factory seems more demanding than, for example, the 130 km baseline considered in Refs. [21,24], we regard this setup as more realistic. Indeed, if a neutrino factory is built, it will need both the 4000 km and the 7500 km baselines in order to have competitive sensitivities to *CP* violation and the mass hierarchy, but it would be too demanding to further divide the flux by adding a third 130 km baseline to study deviations from unitary mixing. Moreover, as we will discuss later, the sensitivities achievable with this setup generally outperform the ones obtained with only the 130 km baseline. On the other hand, it is true that the sensitivities to the new nonunitarity parameters will not depend critically on the presence of the long 7500 km baseline, for instance. However, this baseline is mandatory for the measurement of standard parameters such as δ or the mass hierarchy, which are also allowed to vary in our numerical analysis.

A clean signal of a nonunitary mixing is the presence of ''zero-distance effects'' stemming from the nonorthogonality of the flavor states. Indeed, if the flavor basis is not orthogonal, a neutrino of flavor α can be detected with flavor β without the need of flavor conversion in the propagation. This translates to a baseline-independent term in the oscillation probabilities, which is best probed at short distances, since the flux is larger and it cannot be hidden by the standard oscillations. For short baselines, this term is ($\alpha \neq \beta$)

$$P_{\alpha\beta}(L = 0) = 4|\varepsilon_{\alpha\beta}|^2 + \mathcal{O}(\varepsilon^3). \tag{8}$$

The oscillation probabilities for longer baselines up to second order in the small parameters are derived in Appendix A. Near detectors are thus excellent for probing the zero-distance effect, in particular τ detectors are of importance, since the present bounds on $\varepsilon_{\mu e}$ and $\varepsilon_{\mu\mu}$ are

[3]The anti-Hermitian part can be reabsorbed in the unitary rotation, and is thus related to using different parametrizations.

rather strong. We will therefore study the impact of near τ detectors of different sizes located at 1 km from the beam source. In particular, we will present all the results for near detector sizes of 100 ton, 1 kton, and 10 kton, as well as the results without any near τ detector. Notice that 10 kton is the detector mass discussed for the ECC detector located at 4000 km. However, we have seen no improvement adding such a detector at that baseline while the gain in sensitivity that a near detector capable of τ detection can provide is significant, as we will discuss below. Therefore, we also considered the larger mass to show what could be achieved with the planned 10 kton detector located at 1 km instead of 4000 km. To simulate the near detector, we use the point-source and far-distance approximations. These assumptions are reasonable, although somewhat optimistic in the high-energy region, as can be seen in Fig. 12 of Ref. [37]. However, the loss of flux at higher energies, which corresponds to the on-axis neutrinos, may be recovered by using rather elongated geometries of the near detector. These are precisely the kind of geometries that are being discussed for a magnetized version of the ECC. Such a detector would be limited in size by the above mentioned geometrical considerations and is not likely to be larger than 4 kton. On the other hand, all the decay channels of the τ could be studied in the magnetized version, which would translate into an increase of the efficiency by a factor of 5 with respect to the ECC search for τ decays into μ considered here. The impact of near μ detectors is still essentially to normalize the neutrino flux and cross sections, since the bounds on $\varepsilon_{\mu\mu}$ and $\varepsilon_{\mu e}$ from the unitarity of the CKM matrix and $\mu \to e\gamma$ are particularly strong [19,25].

In our simulations, we will study the ''golden'' [38] $\nu_e \to \nu_\mu$ and ν_μ disappearance channels in the MIND detectors and the ''silver'' [33,34] $\nu_e \to \nu_\tau$ and ''discovery'' [39] $\nu_\mu \to \nu_\tau$ channels at the ECC detectors, both near and far. Since both detector technologies are capable of charge identification and we consider runs with both muon polarities, these channels are considered for both neutrinos and antineutrinos. For the detector efficiencies and backgrounds, we follow the study in Ref. [32] of the MIND detector exposed to the neutrino factory beam. The efficiencies and backgrounds for the silver channel with an ECC detector are carefully discussed in Ref. [34] and we follow the results of that reference. Lacking an analogous study for the discovery channel, we assume the same efficiencies and backgrounds as the ones for the silver channel described in Ref. [34].

For our numerical simulations, we scan the complete MUV parameter space, adding nine unitarity violating parameters to the six standard neutrino oscillation parameters. The scan is performed using the MONTECUBES software [40,41], which allows one to perform Markov Chain Monte Carlo (MCMC) simulations with GLOBES [42,43]. For the implementation of the unitarity deviations in the neutrino oscillation probabilities, we use the NONUNITARITY ENGINE distributed along with the MONTECUBES package. Using the MCMC technique allows the study of possible parameter correlations in the full parameter space without restricting the search to varying only a small subset of the parameters. This is due to the fact that the number of evaluations required by Monte Carlo techniques increases at most polynomially with the number of parameters, while a scan based on grids in the parameter space would require one to evaluate the event rates and likelihoods at a number of points that grows exponentially. For all of our figures, we have used simulations with four MCMC chains containing 2×10^6 samples each. In addition, we have checked that the chains have reached proper convergence, in all cases better than $R - 1 = 10^{-2}$ [44]. It is also important to note that, unlike in the standard usage of the GLOBES software, the use of MCMC techniques is based on Bayesian rather than frequentist parameter estimation and, as such, the result depends on the adopted priors. As priors, we will consider the current bounds on both the standard and the unitarity violating parameters, except for parameters to which the neutrino factory has superior sensitivity, for which we use flat priors.

Before discussing the more detailed studies, let us comment on some of the general results from the simulations. First of all, one of the most remarkable features is that the results do not contain significant correlations between any of the unitarity violating parameters, nor are the unitarity violating parameters significantly correlated with the standard neutrino oscillation parameters. The only exception are some mild correlations between θ_{13}, δ and the modulus and phase of $\varepsilon_{\tau e}$ in the absence of near τ detectors which, however, do not lead to new degeneracies between these parameters or spoil the determination of θ_{13} and δ at the neutrino factory. Furthermore, the addition of a near τ detector of only 100 ton is enough to almost completely erase these correlations. This implies that the neutrino factory setup considered here has enough sensitivity to distinguish the effects induced by unitarity violation from changes in the standard parameters. Second, the sensitivities of the neutrino factory to the diagonal parameters of the ε matrix, as well as to $\varepsilon_{\mu e}$, do not improve with respect to the bounds derived from electroweak decays, which are too stringent to allow for observable effects at the neutrino factory. Notice that none of the oscillation probabilities studied here depend on ε_{ee}, as shown in Appendix A.

We will thus concentrate on the sensitivities to $\varepsilon_{\tau\mu}$ and $\varepsilon_{\tau e}$ in the next subsections, even though the other unitarity violating parameters and standard oscillation parameters are allowed to vary in the simulations. As an example of the sensitivities and correlations to all the 15 parameters considered, the 105 projections to the different two-dimensional subspaces and the marginalized regions for the 15 parameters can be studied in a triangle plot at Ref. [41] for the case of no near τ detector. The input values chosen for the unknown parameters in this example

were $\theta_{13} = 5°$, $\delta = 0$, $|\varepsilon_{\tau e}| = 0.005$, and $\phi_{\tau e} = \pi/4$, the input for the rest of the nonunitary parameters was set to zero. In all our simulations we assume [45,46] $\theta_{12} = 33°$, $\theta_{23} = 45°$, $\Delta m^2_{21} = 8 \cdot 10^{-5}$ eV^2, and $\Delta m^2_{31} = 2.6 \cdot 10^{-3}$ eV^2. We also assumed 4% priors on θ_{12} and Δm^2_{21} at 1σ, flat priors were used for the rest of the standard oscillation parameters. For the unitarity violating parameters, we consider Gaussian priors given by the ranges mentioned in Sec. II.

A. Sensitivity to $\varepsilon_{\tau\mu}$

In the left panel of Fig. 1, we show the sensitivity to the $\varepsilon_{\tau\mu}$ parameter for the four different sizes considered for the near ECC. The input values for all the nonunitarity parameters and θ_{13} were set to zero to derive these curves. We have checked that the results do not depend strongly on this assumption. The most remarkable feature of this figure is the extreme sensitivity to the real part of $\varepsilon_{\tau\mu}$ which is present already without any near detector. This sensitivity mainly originates from the matter effect on the disappearance channel, where the leading nonunitarity correction to the oscillation probability is given by

$$\hat{P}_{\mu\mu} = P^{\mathrm{SM}}_{\mu\mu} - 2\,\mathrm{Re}(\varepsilon_{\mu\tau})AL\sin\left(\frac{\Delta m^2_{31}L}{2E}\right) + \mathcal{O}(\varepsilon_{\mu\mu}), \tag{9}$$

where $A = \sqrt{2}G_F n_e$, the terms we have omitted here can be found in Appendix A. Notice that the discovery channel also depends linearly on $\varepsilon_{\tau\mu}$ and that the dependence is *CP* violating. On the other hand, the mass and efficiency of the ECC detector are much smaller compared to those of the MIND detectors for the ν_μ disappearance channel and therefore the sensitivity is dominated by the latter. As can be seen in the figure, a near τ detector will determine the modulus of $\varepsilon_{\mu\tau}$ through the zero-distance effect. This would translate into a vertical band in the left panel of Fig. 1 and thus the increase of the mass of the near detector improves the measurement of the imaginary part. However, given the linear dependence due to the matter effects on propagation, the bound on the real part from the disappearance channel remains stronger. We can also see that the bound on the modulus does not require a very large near detector, the bound on the imaginary part is essentially only improved by approximately 30% in moving from a 1 kton to a 10 kton ECC detector.

Another important question is how well the neutrino factory would be able to measure the unitarity violating parameters if they are nonzero. For this reason, in Fig. 2, we show the sensitivity to $\varepsilon_{\tau\mu}$ assuming that $|\varepsilon_{\tau\mu}| = 3.2 \cdot 10^{-3}$ as well as $\phi_{\tau\mu} = 45°$ and $-90°$, respectively, which is disfavored at only 1σ by current bounds. Thus, this gives a flavor of the best possible situation for actually discovering unitarity violation and a new source of *CP* violation. Again, we can see that the sensitivity without the near detector is only to the real part of $\varepsilon_{\tau\mu}$. In this setting, there is a degeneracy extending essentially as $|\varepsilon_{\tau\mu}| \propto 1/\cos(\phi_{\tau\mu})$, along which the real part of $\varepsilon_{\tau\mu}$ is constant and the imaginary part is changing. For the case with purely imaginary $\varepsilon_{\tau\mu}$ in the right panel of Fig. 2, it is also no surprise that the results without the near detector are compatible with $\varepsilon_{\tau\mu} = 0$. The introduction of near detectors results in an effective measurement of $|\varepsilon_{\tau\mu}|$, i.e., a vertical band in the plot, which intersects the far detector measurement giving rise to two degenerate solutions, one for positive and one for negative imaginary part. Again, the actual size of the near detector is not crucial and no significant gain is seen beyond 1 kton.

These figures also show the strong complementarity between the near and far detectors when it comes to measuring the phase of the unitarity violating parameter, and thus also a nonstandard source of *CP* violation. Neither the near nor the far detectors alone can establish a *CP*-violating phase by themselves. However, combining the two results excludes *CP* conservation at 90% confidence level, even if a degeneracy on the sign of the *CP*-violating phase remains.

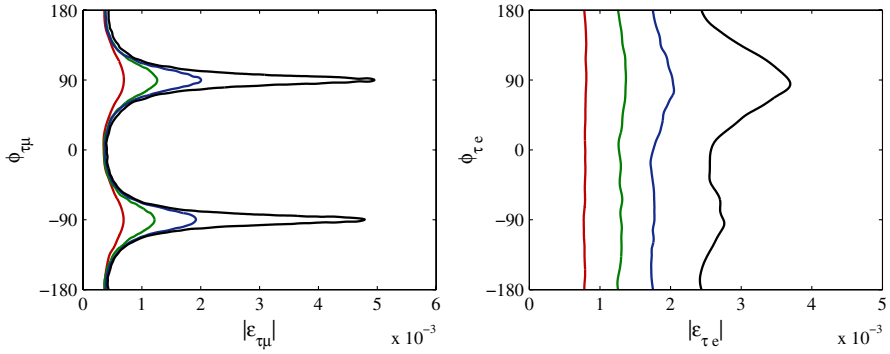

FIG. 1 (color online). The 90% confidence level sensitivity of the IDS neutrino factory to the unitarity violating parameters $\varepsilon_{\tau\mu}$ (left) and $\varepsilon_{\tau e}$ (right). The different curves correspond to different sizes of the near τ detector, from left to right, 10 kton, 1 kton, 100 ton, no near detector.

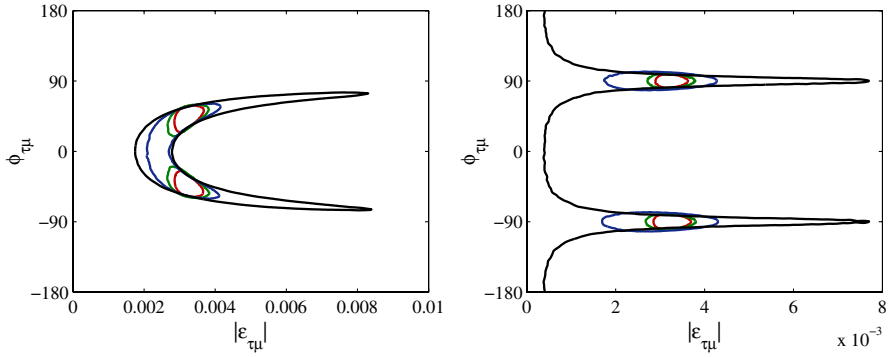

FIG. 2 (color online). The sensitivity of the IDS neutrino factory to the unitarity violating parameter $\varepsilon_{\tau\mu}$, assuming that it takes the value $\varepsilon_{\tau\mu} = 3.2 \cdot 10^{-3} \exp(i\pi/4)$ (left) and $\varepsilon_{\tau\mu} = -i3.2 \cdot 10^{-3}$ (right). The different curves correspond to different sizes of the near τ detector, from inner to outer curves, 10 kton, 1 kton, 100 ton, no near detector.

Note that the slight widening of the allowed region when including the near detector results from the use of Bayesian statistics. Since the near detectors discard a large range of allowed values for $\phi_{\tau\mu}$ when $|\varepsilon_{\tau\mu}|$ is close to zero, a slightly larger region in $\phi_{\tau\mu}$ close to the correct absolute value of $\varepsilon_{\tau\mu}$ is needed in order to include 90% of the probability distribution.

B. Sensitivity to $\varepsilon_{\tau e}$

The right panel of Fig. 1 shows the sensitivity to the unitarity violation parameter $\varepsilon_{\tau e}$ when the input values for θ_{13} and all the unitarity violating parameters are set to zero. Analogously to the sensitivity to $\varepsilon_{\tau\mu}$, the setup with only the far detectors is more sensitive to the real part of the parameter, although the difference is not as pronounced. Furthermore, as can be seen in the oscillation probabilities in Appendix A, the probabilities that depend on $\varepsilon_{\tau e}$ are only the golden, silver, and discovery channels, where the dependence is quadratic rather than linear, which translates into a weaker bound. Thus, the inclusion of the near τ detector has a major impact also on the bound which is placed on the real part of $\varepsilon_{\tau e}$. Indeed, for a 1 kton near τ detector, the sensitivity is essentially flat as a function of $\phi_{\tau e}$ and is dominated by the near detector.

Again, the larger mass and efficiency of the MIND detector compared to the ECC translates into the golden rather than the silver or the discovery channels dominating the sensitivity to $\varepsilon_{\tau e}$ from the far detectors alone. However, unlike the ν_μ disappearance channel, the golden channel is strongly dependent on the unknown parameters θ_{13} and δ and the input values assumed for them will influence the expected sensitivity to $\varepsilon_{\tau e}$. Indeed, the $\nu_e \to \nu_\mu$ probability in the presence of nonunitarity is modified to

$$\begin{aligned}\hat{P}_{e\mu} = P_{e\mu}^{\mathrm{SM}} &+ |\varepsilon_{e\tau}|^2 \sin^2\left(\frac{E_3 L}{2}\right) + \mathrm{Im}\left\{\varepsilon_{e\tau}\left[\frac{1}{2}\frac{E_2}{A}\sin(2\theta_{12}) + \frac{E_3 s_{13} e^{i\delta}}{A - E_3}\right]\right\} \sin\left(\frac{AL}{2}\right)\sin\left(\frac{E_3 L}{2}\right)\sin\left(\frac{E_3 - A}{2}L\right) \\ &+ \mathrm{Re}\left\{\varepsilon_{e\tau}\left[\frac{1}{\sqrt{2}}\frac{E_2}{A}\sin(2\theta_{12})\sin\left(\frac{AL}{2}\right)\cos\left(\frac{E_3 - A}{2}L\right) - \frac{2\sqrt{2} E_3 s_{13} e^{i\delta}}{A - E_3}\cos\left(\frac{AL}{2}\right)\sin\left(\frac{E_3 - A}{2}L\right)\right]\right\}\sin\left(\frac{E_3 L}{2}\right) \\ &+ \mathcal{O}(\varepsilon^3), \end{aligned} \tag{10}$$

where $E_i = \Delta m_{i1}^2/(2E)$. It is then clear that the relative importance of the real and imaginary parts of $\varepsilon_{\tau e}$ in this probability strongly depends on the actual values of θ_{13} and δ. As an example of this dependence, in Fig. 3, we again show the sensitivity to $\varepsilon_{\tau e}$, but for input values of $\theta_{13} = 5°$ as well as for $\delta = \pi/4$ (left panel) and $\delta = 0$ (right panel). Notice that while for $\delta = \pi/4$ the far MIND detectors are more sensitive to the imaginary part of $\varepsilon_{\tau e}$ the situation is reversed for $\delta = 0$. However, the addition of the near τ detector for the silver channel dominates the bound and the curves incorporating the near detectors forecast the same sensitivity regardless of the true values of θ_{13} and δ.

In Fig. 4, we show the analogue of Fig. 2 for $\epsilon_{\tau e}$. In this case, we assume $|\varepsilon_{\tau e}| = 5.0 \cdot 10^{-3}$ and $\phi_{\tau e} = 45°$ and $-90°$, which again corresponds to the 1σ disfavored region. For this example, CP violation would not be discovered for the $\phi_{\tau e} = 45°$ case (left panel) at the 90% CL, but it would be constrained around its true value already by the far detectors. In addition, the inclusion of a near τ detector would again constrain the modulus and therefore be complementary to the far detector result. For the $\phi_{\tau e} = -90°$

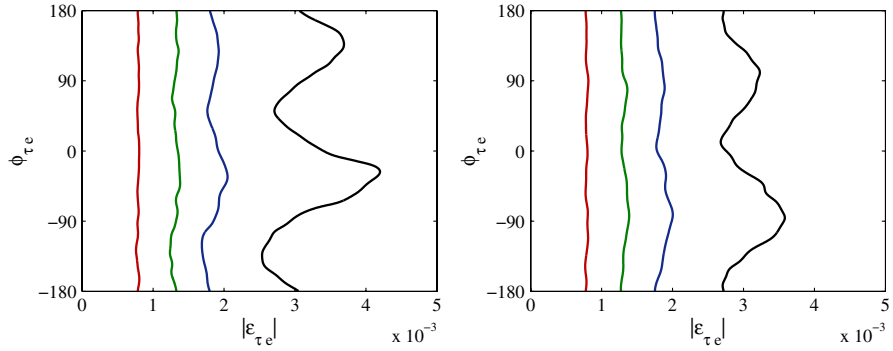

FIG. 3 (color online). The 90% confidence level sensitivity of the IDS neutrino factory to the unitarity violating parameter $\varepsilon_{\tau e}$ with $\theta_{13} = 5°$ as well as $\delta = \pi/4$ (left) and $\delta = 0$ (right). The different curves correspond to different sizes of the near τ detector, from left to right, 10 kton, 1 kton, 100 ton, no near detector.

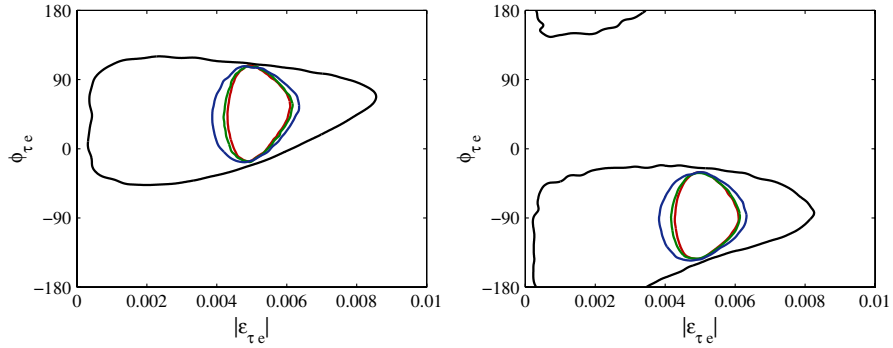

FIG. 4 (color online). The sensitivity of the IDS neutrino factory to the unitarity violating parameter $\varepsilon_{\tau e}$, assuming that it takes the value $\varepsilon_{\tau e} = 5.0 \cdot 10^{-3} \exp(i\pi/4)$ (left) and $\varepsilon_{\tau\mu} = -i5.0 \cdot 10^{-3}$ (right). The different curves correspond to different sizes of the near τ detector, from inner to outer curves, 10 kton, 1 kton, 100 ton, no near detector.

case (right panel), the complementarity of the near and far detectors is able to exclude *CP* conservation at the 90% CL.

IV. SUMMARY AND DISCUSSION

We have considered the sensitivity of the IDS Neutrino Factory setup to minimal unitarity violation (MUV) by using the Markov Chain Monte Carlo methods implemented in MONTECUBES to explore the full parameter space, consisting of the six standard neutrino oscillation parameters and nine additional parameters describing the deviation from unitarity. Our simulations were performed with several different near ECC τ detector setups, ranging from no near detector to near detector masses up to 10 kton.

Our results imply that the neutrino factory will be excellent for probing some of the unitarity violating parameters. In particular, a sensitivity of $\mathcal{O}(10^{-4})$ to the real part of the unitarity violating parameter $\varepsilon_{\tau\mu}$ is found. This is mainly due to the matter effects in the ν_μ disappearance channel at the far detectors, for which the oscillation probability is only linearly suppressed in $\mathrm{Re}(\varepsilon_{\tau\mu})$. On the other hand, we find that a near τ detector with a mass as small as 100 ton would dominate the sensitivity to $\varepsilon_{\tau e}$, as well as that to the imaginary part of $\varepsilon_{\tau\mu}$, through the measurement of the zero-distance effect, providing sensitivities down to $\mathcal{O}(10^{-3})$. For the other unitarity violating parameters, we recover the priors of our simulation, which were set to the current experimental bounds. The setup studied here will therefore not improve our present knowledge of them.

Furthermore, we find no degeneracies neither among the different unitarity violating parameters, nor between the unitarity violating parameters and the small standard neutrino oscillation parameters, such as θ_{13}. This means that the sensitivities to the standard oscillation parameters are robust even in presence of unitarity violation.

Regarding the prospects of an actual detection of unitarity violation, and especially *CP*-violation stemming from nonunitary mixing, we find that the near and far detectors play a very complementary role. In the case of $\varepsilon_{\tau\mu}$, the far detectors are only sensitive to the real part of the unitarity violating parameter while the near detector can measure its modulus, neither is sensitive to unitarity violating *CP* violation by themselves. However, it can be

effectively probed by considering the combination of the two, as illustrated in Fig. 2.

We would like to stress that, while the sensitivity to unitarity violation at a neutrino factory has been studied before [21,24,26,28,47], the sensitivity to the real part of $\varepsilon_{\tau\mu}$ due to matter effects in the ν_μ disappearance channel has not been discussed (however, a similar term is present in and has been studied for the case of oscillations into sterile neutrinos [39]). Furthermore, these studies have not systematically scanned the parameter space while keeping all parameters free within their prior values. Thus, the observation that there are no extended degeneracies, neither between the standard and unitarity violating parameters, nor among the unitarity violating parameters themselves, is also new.

We conclude that a neutrino factory would provide powerful tool for probing unitarity violation in the leptonic mixing matrix. For the parameters to which it is most sensitive, the sensitivity is an order of magnitude better than the current experimental bounds. Finally, the interplay between the near and far detectors would allow one to test new sources of CP violation in the lepton sector.

ACKNOWLEDGMENTS

We would like to thank A. Donini, W. Wang, and Z.-z. Xing for useful discussions. This work was supported by the Swedish Research Council (Vetenskapsrådet), Contract No. 623-2007-8066 [M. B.]. S. A., M. B., and E. F. M. acknowledge support by the DFG cluster of excellence ''Origin and Structure of the Universe.'' J. L. P. acknowledges financial support by the Ministry of Science and Innovation of Spain (MICIINN) through an FPU Grant Ref. No. AP2005-1185. S. A., E. F. M., and J. L. P. also acknowledge support from the European Community under the European Commission Framework Programme 7 Design Study: EUROnu, Project No. 212372.

APPENDIX: OSCILLATION PROBABILITIES IN THE PRESENCE OF UNITARITY VIOLATION

In this appendix, we derive the probabilities $P_{\alpha\beta}$ in matter assuming constant density. In order to perform the calculation, we will use the Kimura-Takamura-Yokomura (KTY) formalism [48,49], which has already been applied to the MUV scheme in the appendix of Ref. [21]. Since the constraint on $\varepsilon_{e\mu}$ is strong enough to safely neglect $\varepsilon_{e\mu}$ in the oscillation probabilities, we will not consider it below. However, it has been considered in the numerical analysis presented in the main part of this paper. The effective flavor eigenstates are given by

$$|\nu_\alpha\rangle = \frac{(1+\varepsilon^*)_{\alpha\beta} U^*_{\beta i}}{[1+2\varepsilon_{\alpha\alpha}+(\varepsilon^2)_{\alpha\alpha}]^{1/2}}|\nu_i\rangle \equiv \frac{(1+\varepsilon^*)_{\alpha\beta}}{[1+2\varepsilon_{\alpha\alpha}+(\varepsilon^2)_{\alpha\alpha}]^{1/2}}|\nu^{\rm SM}_\beta\rangle. \quad \text{(A1)}$$

The parameters that appear linearly in the normalization factors are ε_{ee}, $\varepsilon_{\mu\mu}$, and $\varepsilon_{\tau\tau}$, which are already better constrained by other considerations than the sensitivities we find for a neutrino factory. Thus, the determination of the fluxes and cross sections by the near detectors only suffer from a minor additional theoretical uncertainty. We will present the oscillation probabilities $\hat{P}(\nu_\alpha \to \nu_\beta) = \hat{P}_{\alpha\beta}$ without taking the normalization factors into account. Notice that this will not be at all relevant for the golden and silver channels, since the probabilities are already order ε^2 before taking the normalization factors into account. Thus, the corrections would be at most $\mathcal{O}(\varepsilon^3)$.

The oscillation probability $\hat{P}_{\alpha\beta}$, expressed as a function of the KTY parameters, is [21]

$$\hat{P}_{\alpha\beta} = |(NN^\dagger)_{\alpha\beta}|^2 - 4\sum_{j<k}\mathrm{Re}(\tilde{X}^{\alpha\beta}_j \tilde{X}^{\alpha\beta *}_k)\sin^2\left(\frac{\Delta\tilde{E}_{jk}L}{2}\right) + 2\sum_{j<k}\mathrm{Im}(\tilde{X}^{\alpha\beta}_j \tilde{X}^{\alpha\beta *}_k)\sin(\Delta\tilde{E}_{jk}L), \quad \text{(A2)}$$

where $\Delta\tilde{E}_{jk} \equiv \tilde{E}_j - \tilde{E}_k$ and $\tilde{X}^{\alpha\beta}_j \equiv (N^* W)_{\alpha j}(N^* W)^*_{\beta j}$ ($j = 1, 2, 3$). Here, $\tilde{E}_i$ are the effective eigenvalues in matter and W_{ij} is the unitary matrix which diagonalizes the evolution equation for the mass eigenstates:

$$i\frac{d}{dt}|\nu_i\rangle = [\mathrm{diag}(E_1, E_2, E_3) + N^\dagger \sqrt{2} G_F \times \mathrm{diag}(n_e - n_n/2, -n_n/2, -n_n/2) N]_{ji}|\nu_j\rangle \equiv \mathcal{H}_{ji}|\nu_j\rangle, \quad \text{(A3)}$$

where $E_i = \Delta m^2_{i1}/(2E)$. Assuming that the electron and neutron number densities are equal[4] (i.e., $n_e = n_n$), $\mathcal{H}$ can be expressed as

$$\mathcal{H} = \mathrm{diag}(E_1, E_2, E_3) + N^\dagger \mathrm{diag}\left(\frac{A}{2}, -\frac{A}{2}, -\frac{A}{2}\right) N, \quad \text{(A4)}$$

where $A = \sqrt{2} G_F n_e$. Finally, according to the KTY formalism applied to the MUV scheme (again, see Ref. [21]), $\tilde{X}^{\alpha\beta}_j$ can be expressed as

$$\tilde{X}^{\alpha\beta}_j \equiv \sum_l (V^{-1})_{jl} Y^{\alpha\beta}_l = \sum_l (V^{-1})_{jl} [N \mathcal{H}^{l-1} N^\dagger]_{\beta\alpha}, \quad \text{(A5)}$$

where

$$V^{-1} = \begin{pmatrix} (\Delta\tilde{E}_{21}\Delta\tilde{E}_{31})^{-1}(\tilde{E}_2\tilde{E}_3, -\tilde{E}_2 - \tilde{E}_3, 1) \\ -(\Delta\tilde{E}_{21}\Delta\tilde{E}_{32})^{-1}(\tilde{E}_3\tilde{E}_1, -\tilde{E}_3 - \tilde{E}_1, 1) \\ (\Delta\tilde{E}_{31}\Delta\tilde{E}_{32})^{-1}(\tilde{E}_2\tilde{E}_1, -\tilde{E}_2 - \tilde{E}_1, 1) \end{pmatrix}. \quad \text{(A6)}$$

Once the effective eigenvalues in matter are known, it is

[4]This is a very good approximation in the case of neutrino oscillations in the Earth.

straightforward to obtain the expressions for the neutrino oscillation probabilities. However, in order to obtain reasonably simple expressions, it is necessary to expand them in small parameters. Here, we present the oscillation probabilities to second order in the parameters listed in Table I.

To second order in ε, we can find the eigenvalues by using perturbation theory. We find that

$$\tilde{E}_1 = A\Big[1 + \frac{E_2}{A}s_{12}^2 + \frac{1}{4}\frac{E_2^2}{A^2}\sin^2(2\theta_{12}) + \frac{E_3 s_{13}^2}{A - E_3} + \varepsilon_{ee} + \frac{\varepsilon_{ee}^2}{2} - \frac{|\varepsilon_{e\tau}|^2}{2}\Big] + \mathcal{O}(\varepsilon^3), \tag{A7}$$

$$\tilde{E}_2 = A\Big\{\frac{E_2}{A}c_{12}^2 - \frac{E_2^2}{4A^2}\sin^2(2\theta_{12}) + \mathrm{Re}(\varepsilon_{\mu\tau})\Big[1 + \frac{1}{2}(\varepsilon_{\mu\mu} + \varepsilon_{\tau\tau})\Big] - \frac{1}{2}(\varepsilon_{\mu\mu} + \varepsilon_{\tau\tau}) - \frac{1}{4}(\varepsilon_{\mu\mu}^2 + \varepsilon_{\tau\tau}^2) - \frac{|\varepsilon_{\mu\tau}|^2}{2} + \frac{|\varepsilon_{e\tau}|^2}{4} - \delta\theta_{23}\Big[\varepsilon_{\tau\tau} - \varepsilon_{\mu\mu} + \frac{1}{2}(\varepsilon_{\tau\tau}^2 - \varepsilon_{\mu\mu}^2) - |\varepsilon_{e\tau}|^2/2\Big] - \frac{A}{E_3}\mathrm{Re}(\varepsilon_{\mu\tau})^2 - \frac{A}{4E_3}(\varepsilon_{\tau\tau} - \varepsilon_{\mu\mu})^2\Big\} + \mathcal{O}(\varepsilon^3), \tag{A8}$$

$$\tilde{E}_3 = A\Big\{\frac{E_3}{A} - \frac{E_3 s_{13}^2}{A - E_3} - \mathrm{Re}(\varepsilon_{\mu\tau})\Big[1 + \frac{1}{2}(\varepsilon_{\mu\mu} + \varepsilon_{\tau\tau})\Big] + \delta\theta_{23}(\varepsilon_{\tau\tau} - \varepsilon_{\mu\mu}) - \frac{1}{2}(\varepsilon_{\mu\mu} + \varepsilon_{\tau\tau}) - \frac{1}{4}(\varepsilon_{\tau\tau}^2 + \varepsilon_{\mu\mu}^2) - \frac{|\varepsilon_{\mu\tau}|^2}{2} + \frac{|\varepsilon_{e\tau}|^2}{4}\Big\} + \mathcal{O}(\varepsilon^3). \tag{A9}$$

TABLE I. The small expansion parameters used in our neutrino oscillation probabilities. We will refer to the set of SM expansion parameters as η. The full set of expansion parameters will be referred to as ε, while only the set of MUV expansion parameters will be denoted by $\varepsilon_{\alpha\beta}$.

SM expansion parameters (η)	MUV expansion parameters
θ_{13}, $\Delta m_{21}^2/\Delta m_{31}^2$, $\delta\theta_{23} = \theta_{23} - \pi/4$	$\varepsilon_{\alpha\beta}$

Notice that, for $\varepsilon_{\alpha\beta} \to 0$, we recover the SM results as expected. These results allow us to obtain V^{-1} at second order. Thus, we only need to compute $Y_j^{\alpha\beta}$ at the same order, the computation is straightforward but tedious [see Eq. (A5)]. For brevity, we do not present the results for V^{-1} and $Y_j^{\alpha\beta}$ here. However, we would like to comment that, for the golden and silver channels, it is enough to compute these quantities to first order, since $\tilde{X}_j^{\alpha\beta}$ is already of first order in η. This is not true in the case of the ν_μ-ν_τ sector, where $\tilde{X}_2^{\mu\mu}|_{\varepsilon=0} = \tilde{X}_3^{\mu\mu}|_{\varepsilon=0} = -\tilde{X}_2^{\tau\mu}|_{\varepsilon=0} = \tilde{X}_3^{\tau\mu}|_{\varepsilon=0} = 1/2$. The advantage of this sector, from the point of view of discovering new physics, is that the effects of the new physics can appear in the probability at first order as an interference term between the SM and the new physics without additional suppression by η. For this reason, we keep only the interference between the $\mathcal{O}(\varepsilon_{\alpha\beta})$ terms and the $\mathcal{O}(\eta)$ ones at second order[5] in that sector.

In the end, we obtain the following expanded oscillation probabilities at the orders mentioned above:

$$\hat{P}_{\mu\mu} = P_{\mu\mu}^{\mathrm{SM}} + 4\varepsilon_{\mu\mu} + 4\varepsilon_{\mu\mu}^2 + 4\Big\{-\varepsilon_{\mu\mu} + 2\,\mathrm{Re}(\varepsilon_{\mu\tau})\delta\theta_{23} - 2\delta\theta_{23}(\varepsilon_{\mu\mu} - \varepsilon_{\tau\tau})\frac{A}{E_3}\Big\}\sin^2\Big(\frac{E_3 L}{2}\Big) - [2\,\mathrm{Re}(\varepsilon_{\mu\tau}) - \delta\theta_{23}(\varepsilon_{\mu\mu} - \varepsilon_{\tau\tau})]AL\sin(E_3 L) + \mathcal{O}(\varepsilon_{\alpha\beta}^2), \tag{A10}$$

$$\hat{P}_{\mu\tau} = P_{\mu\tau}^{\mathrm{SM}} + 4|\varepsilon_{\mu\tau}|^2 + \Big[2\,\mathrm{Re}(\varepsilon_{\mu\mu} + \varepsilon_{\tau\tau}) + 8\delta\theta_{23}(\varepsilon_{\mu\mu} - \varepsilon_{\tau\tau})\frac{A}{E_3}\Big]\sin^2\Big(\frac{E_3 L}{2}\Big) + [-2\,\mathrm{Im}(\varepsilon_{\mu\tau}) - \delta\theta_{23}(\varepsilon_{\mu\mu} - \varepsilon_{\tau\tau})AL] \times \sin(E_3 L) - \sqrt{2}\,\mathrm{Im}\Big\{\varepsilon_{e\tau}\Big[\frac{E_2}{A}\sin(2\theta_{12}) + \frac{2E_3 s_{13}e^{i\delta}}{A - E_3}\Big]\Big\}\sin\Big(\frac{AL}{2}\Big)\sin\Big(\frac{E_3 L}{2}\Big)\sin\Big(\frac{E_3 - A}{2}L\Big) + \sqrt{2}\,\mathrm{Re}\Big\{\varepsilon_{e\tau}\Big[\frac{E_2}{A}\sin(2\theta_{12})\sin\Big(\frac{AL}{2}\Big)\cos\Big(\frac{E_3 - A}{2}L\Big) - \frac{2E_3 s_{13}e^{i\delta}}{A - E_3}\cos\Big(\frac{AL}{2}\Big)\sin\Big(\frac{E_3 - A}{2}L\Big)\Big]\Big\}\sin\Big(\frac{E_3 L}{2}\Big) + \mathcal{O}(\varepsilon_{\alpha\beta}^2), \tag{A11}$$

[5]It could also be justified to neglect the $\mathcal{O}(\varepsilon_{\alpha\beta}\frac{\Delta m_{21}^2}{\Delta m_{31}^2})$ terms, since the maximal allowed value of $\frac{\Delta m_{21}^2}{\Delta m_{31}^2}$ is at least 1 order of magnitude smaller than the maximal allowed values of s_{13} and $\delta\theta_{23}$. However, we keep also these terms for completeness.

$$\hat{P}_{e\mu} = P^{\rm SM}_{e\mu} + |\varepsilon_{e\tau}|^2 \sin^2\left(\frac{E_3 L}{2}\right) + {\rm Im}\left\{\varepsilon_{e\tau}\left[\frac{1}{2}\frac{E_2}{A}\sin(2\theta_{12}) + \frac{E_3 s_{13} e^{i\delta}}{A - E_3}\right]\right\} \sin\left(\frac{AL}{2}\right)\sin\left(\frac{E_3 L}{2}\right)\sin\left(\frac{E_3 - A}{2}L\right)$$
$$+ {\rm Re}\left\{\varepsilon_{e\tau}\left[\frac{1}{\sqrt{2}}\frac{E_2}{A}\sin(2\theta_{12})\sin\left(\frac{AL}{2}\right)\cos\left(\frac{E_3 - A}{2}L\right) - \frac{2\sqrt{2}E_3 s_{13} e^{i\delta}}{A - E_3}\cos\left(\frac{AL}{2}\right)\sin\left(\frac{E_3 - A}{2}L\right)\right]\right\}\sin\left(\frac{E_3 L}{2}\right)$$
$$+ \mathcal{O}(\varepsilon^3), \tag{A12}$$

$$\hat{P}_{e\tau} = P^{\rm SM}_{e\tau} + 4|\varepsilon_{e\tau}|^2 - 2\left[|\varepsilon_{e\tau}|^2 - \frac{\sqrt{2}E_3 s_{13}}{A - E_3}{\rm Re}(\varepsilon_{e\tau} e^{i\delta})\right]\sin^2\left(\frac{E_3 - A}{2}L\right) - 2\left[|\varepsilon_{e\tau}|^2 - \frac{1}{\sqrt{2}}\frac{E_2}{A}\sin(2\theta_{12}){\rm Re}(\varepsilon_{e\tau})\right]$$
$$\times \sin^2\left(\frac{AL}{2}\right) - {\rm Im}\left\{\varepsilon^*_{e\tau}\left[\frac{1}{\sqrt{2}}\frac{E_2}{A}\sin(2\theta_{12})\sin(AL) - \frac{\sqrt{2}E_3 s_{13} e^{-i\delta}}{A - E_3}\sin(\{E_3 - A\}L)\right]\right\}$$
$$- 2\sqrt{2}\,{\rm Re}\left\{\varepsilon_{e\tau}\left[\frac{1}{2}\frac{E_2}{A}\sin(2\theta_{12}) - \frac{E_3 s_{13} e^{i\delta}}{A - E_3}\right]\right\}\sin\left(\frac{AL}{2}\right)\cos\left(\frac{E_3 L}{2}\right)\sin\left(\frac{E_3 - A}{2}L\right)$$
$$+ {\rm Im}\left\{\varepsilon_{e\tau}\left[\sqrt{2}\frac{E_2}{A}\sin(2\theta_{12})\sin\left(\frac{AL}{2}\right)\cos\left(\frac{E_3 - A}{2}L\right) + \frac{2\sqrt{2}E_3 s_{13} e^{i\delta}}{A - E_3}\cos\left(\frac{AL}{2}\right)\sin\left(\frac{E_3 - A}{2}L\right)\right]\right\}\cos\left(\frac{E_3 L}{2}\right) + \mathcal{O}(\varepsilon^3). \tag{A13}$$

Notice that we do not neglect the zero-distance effect in the ν_μ-ν_τ sector. Although this is not within the order of the expansion, we keep it as it plays an important role in the analysis of the neutrino flavour transitions at near detectors.

[1] S. Geer, Phys. Rev. D **57**, 6989 (1998).
[2] A. De Rujula, M. B. Gavela, and P. Hernandez, Nucl. Phys. **B547**, 21 (1999).
[3] P. Minkowski, Phys. Lett. **67B**, 421 (1977).
[4] M. Gell-Mann, P. Ramond, and R. Slansky, in *Supergravity*, edited by P. van Nieuwenhuizen and D. Freedman (North-Holland, Amsterdam, 1979), p. 315.
[5] T. Yanagida, in *Proceedings of the Workshop on the Unified Theory and the Baryon Number in the Universe*, edited by O. Sawada and A. Sugamoto (Natl. Lab. High Energy Phys., Tsukuba, 1979) KEK Report No. 79–18, p. 95.
[6] R. N. Mohapatra and G. Senjanovic, Phys. Rev. Lett. **44**, 912 (1980).
[7] J. Schechter and J. W. F. Valle, Phys. Rev. D **22**, 2227 (1980).
[8] J. Schechter and J. W. F. Valle, Phys. Rev. D **25**, 774 (1982).
[9] P. Langacker and D. London, Phys. Rev. D **38**, 886 (1988).
[10] S. M. Bilenky and C. Giunti, Phys. Lett. B **300**, 137 (1993).
[11] E. Nardi, E. Roulet, and D. Tommasini, Phys. Lett. B **327**, 319 (1994).
[12] D. Tommasini, G. Barenboim, J. Bernabeu, and C. Jarlskog, Nucl. Phys. **B444**, 451 (1995).
[13] S. Bergmann and A. Kagan, Nucl. Phys. **B538**, 368 (1999).
[14] M. Czakon, J. Gluza, and M. Zralek, Acta Phys. Pol. B **32**, 3735 (2001).
[15] B. Bekman, J. Gluza, J. Holeczek, J. Syska, and M. Zralek, Phys. Rev. D **66**, 093004 (2002).
[16] W. Loinaz, N. Okamura, T. Takeuchi, and L. C. R. Wijewardhana, Phys. Rev. D **67**, 073012 (2003).
[17] W. Loinaz, N. Okamura, S. Rayyan, T. Takeuchi, and L. C. R. Wijewardhana, Phys. Rev. D **68**, 073001 (2003).
[18] W. Loinaz, N. Okamura, S. Rayyan, T. Takeuchi, and L. C. R. Wijewardhana, Phys. Rev. D **70**, 113004 (2004).
[19] S. Antusch, C. Biggio, E. Fernandez-Martinez, M. B. Gavela, and J. Lopez-Pavon, J. High Energy Phys. 10 (2006) 084.
[20] A. Abada, C. Biggio, F. Bonnet, M. B. Gavela, and T. Hambye, J. High Energy Phys. 12 (2007) 061.
[21] E. Fernandez-Martinez, M. B. Gavela, J. Lopez-Pavon, and O. Yasuda, Phys. Lett. B **649**, 427 (2007).
[22] J. Holeczek, J. Kisiel, J. Syska, and M. Zralek, Eur. Phys. J. C **52**, 905 (2007).
[23] Z.-z. Xing, Phys. Lett. B **660**, 515 (2008).
[24] S. Goswami and T. Ota, Phys. Rev. D **78**, 033012 (2008).
[25] S. Antusch, J. P. Baumann, and E. Fernandez-Martinez, Nucl. Phys. **B810**, 369 (2009).
[26] G. Altarelli and D. Meloni, Nucl. Phys. **B809**, 158 (2009).
[27] Z.-z. Xing, arXiv:0902.2469.
[28] M. Malinsky, T. Ohlsson, and H. Zhang, Phys. Rev. D **79**, 073009 (2009).
[29] A. Broncano, M. B. Gavela, and E. E. Jenkins, Phys. Lett. B **552**, 177 (2003).
[30] A. Bandyopadhyay *et al.* (ISS Physics Working Group), arXiv:0710.4947.
[31] IDS Working Group, https://www.ids-nf.org/wiki/FrontPage.
[32] T. Abe *et al.* (ISS Detector Working Group), JINST **4**, T05001 (2009).

[33] A. Donini, D. Meloni, and P. Migliozzi, Nucl. Phys. **B646**, 321 (2002).
[34] D. Autiero *et al.*, Eur. Phys. J. C **33**, 243 (2004).
[35] J. Burguet-Castell, M. B. Gavela, J. J. Gomez-Cadenas, P. Hernandez, and O. Mena, Nucl. Phys. **B608**, 301 (2001).
[36] P. Huber and W. Winter, Phys. Rev. D **68**, 037301 (2003).
[37] J. Tang and W. Winter, arXiv:0903.3039.
[38] A. Cervera *et al.*, Nucl. Phys. **B579**, 17 (2000).
[39] A. Donini, K.-i. Fuki, J. Lopez-Pavon, D. Meloni, and O. Yasuda, arXiv:0812.3703.
[40] M. Blennow and E. Fernandez-Martinez, arXiv: 0903.3985.
[41] M. Blennow and E. Fernandez-Martinez, MONTECUBES, http://wwwth.mppmu.mpg.de/members/blennow/montecubes/.
[42] P. Huber, M. Lindner, and W. Winter, Comput. Phys. Commun. **167**, 195 (2005).
[43] P. Huber, J. Kopp, M. Lindner, M. Rolinec, and W. Winter, Comput. Phys. Commun. **177**, 432 (2007).
[44] A. Gelman and D. Rubin, Stat. Sci. **7**, 457 (1992).
[45] M. Maltoni, T. Schwetz, M. A. Tortola, and J. W. F. Valle, New J. Phys. **6**, 122 (2004).
[46] M. C. Gonzalez-Garcia and M. Maltoni, Phys. Rep. **460**, 1 (2008).
[47] M. Campanelli and A. Romanino, Phys. Rev. D **66**, 113001 (2002).
[48] K. Kimura, A. Takamura, and H. Yokomakura, Phys. Rev. D **66**, 073005 (2002).
[49] O. Yasuda, arXiv:0704.1531.